Modeling and Delay Analysis of Intermittent V2U Communication in Secluded Areas

Maurice Khabbaz, *Senior Member, IEEE*, Joseph Antoun, *Member, IEEE*, Sanaa Sharafeddine, *Senior Member, IEEE*, and Chadi Assi, *Fellow, IEEE*

***Abstract*— This paper investigates the data-delivery latency in the context of intermittent vehicle-to-UAV (V2U) communications. Precisely, a V2U communication scenario is considered where vehicles opportunistically establish connectivity with passing by UAVs for a limited period of time during which these vehicles transmit data packets to in-range UAVs serving as flying base stations and, in turn, are responsible for delivering these packets to backbone networks and/or routing them over the Internet. A mathematical framework is established with the objective of modeling the vehicles' OnBoard Units' (OBUs') buffers as single-server queueing systems. The established queueing model will allow for the evaluation of the V2U communication system in terms of the average data packet delivery delay. Extensive simulations are conducted with the objective of asserting the validity and accuracy of the proposed queueing model as well as providing further insights into the delay sensibility to various system parameters.**

***Index Terms*— IoT, UAV, IoV, vehicular, modeling.**

I. Introduction

A. Preliminaries

GIVEN their flexibility, high mobility, altitude adaptiveness, line-of-sight and so many other characteristics, aerial platforms (*e.g.* Unmanned Aerial Vehicles (UAVs) *a.k.a.* drones, helikites, balloons, etc) present themselves as propitious solutions for provisioning reliable and cost-effective wireless access for ground-based devices. These UAVs, when equipped with appropriate wireless communication devices and computerized modules, may serve as airborne base stations to expand coverage and enhance the capacity of terrestrial wireless networks. especially in emergency situations where, often, ground networking infrastructure is highly likely to be damaged and/or unfunctional as well as in geographically restricted areas where the deployment and maintenance of ground-based networking infrastructure incurs significant capital and operational expenditures, [1]–[8]. Indeed, one of the pivotal advantages of intelligent UAVs (*e.g.*, Google Loon project [9], Boeing's HALE [10], Airbus's Zephyr [11]) is their sui generis capability of provisioning fast, reliable and cost-efficient connectivity to merely isolated areas (*e.g.* rural and suburban areas, large inter-metropolitan highways, developing areas, etc). Yet, regardless of the potential data communication welfare that UAVs bring upfront to a multitude of practical applications, there exist several technical challenges (*e.g.* flight optimization, energy consumption, deployment, user association, communication protocols, latency/throughput performance, etc) that need to be resolved before full-fledged aerial data networking backbones observe light.

B. Motivation and Problem Statement

Intelligent Transportation Systems (ITSs) constitute, today, one of the integral industry verticals of the next generation wireless networks. Newly manufactured vehicles are being equipped with modern ubiquitous technology (*e.g.* processing units, AI modules, wireless communication devices, electronic sensors, actuators, etc) with the objective of mediating ITSs' physical and digital layers; hence, supporting the proper functionality of the numerous novel in-transit services that go beyond the typical data collection and exchange through Vehicle-to-Vehicle (V2V) and Vehicle-to-Infrastructure (V2I) communications. Truly, a new Vehicle-to-Everything (V2E) communication paradigm is being brought forward. It promotes vehicles' real-time awareness of their navigational environment and their ability to cooperate distributively and autonomously with surrounding devices in order to provide passengers with an unparalleled travel experience.

In addition to smart vehicles, an ITS's digital networking infrastructure comprises another type of stationary nodes strategically deployed along the sides of navigable driveways, namely, the RoadSide Units (RSUs). Similar to the vehicles, RSUs are wireless devices typically equipped with processing modules and buffering capabilities. Some of these RSUs may be connected to wireless backhauls enabling them to host a number of vital ITS services that they provision to vehicles navigating within their communication range. Such services include but are not limited to: *a*) on-the-fly streaming of high-quality interruption-free media, [12], *b*) seamless vehicular mobility, [13], *c*) field-limited emergency support and rescuing services, [14], *d*) traffic monitoring and roadway surveying, [15], *e*) improved data routing and dissemination, [16], *e*) vehicular cloud-based services, [17], *f*) safety-related

Manuscript received November 6, 2019; revised January 25, 2020; accepted February 3, 2020. Date of publication February 12, 2020; date of current version May 8, 2020. This work was supported by Concordia University/FQRNT. The associate editor coordinating the review of this article and approving it for publication was G. Fodor. *(Corresponding author: Maurice Khabbaz.)*

Maurice Khabbaz is with the ECCE Department, Notre Dame University of Louaizeh, Zouk Mosbeh 72, Lebanon (e-mail: mkhabbaz@ndu.edu.lb).

Joseph Antoun and Chadi Assi are with the ECE/CIISE Departments, Concordia University, Montreal, QC H3G 1M8, Canada (e-mail: j.antoun89@hotmail.com; assi@ciise.concordia.ca).

Sanaa Sharafeddine is with the CSM Department, Lebanese American University, Beirut 13-5053, Lebanon (e-mail: sanaa.sharafeddine@lau.edu.lb).

Color versions of one or more of the figures in this article are available online at http://ieeexplore.ieee.org.

Digital Object Identifier 10.1109/TWC.2020.2971976

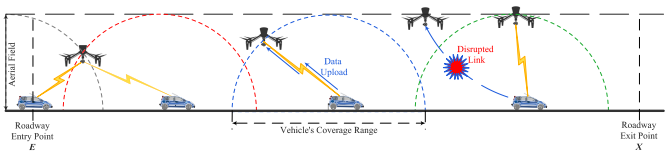

Fig. 1. Vehicle-to-UAV communication along a dark roadway.

services (*e.g.* see through downstream vehicles, [32]) and so many others. Such services vociferate a surge for an all-time-anywhere connectivity to the wireless infrastructure. This latter, is, however, not always feasible particularly in some areas where the deployment of RSUs is geographically restricted as well as in severe environments and along large intra-/inter-national highways where the installation and maintenance of backbone networking infrastructure incurs significant capital and operational expenditures. In the context of such restrictive scenarios, UAVs present themselves as a promising cost-minimal and effective solution for bringing digital connectivity to vehicles navigating along dark roadways. For instance, Figure 1 herein illustrates a dark roadway segment (*i.e.* with no RSUs deployed along its sides) labelled $[EX]$ with E and X being its entry and exit points respectively. Throughout their navigation period along $[EX]$, vehicles are fully disconnected from any backbone network. Consequently, aside from their ability to inter-communicate for real-time navigation or safety-related information exchange, vehicles are deprived from any Internet/Cloud-based services such as those mentioned earlier. Under such circumstances, incoming intelligent UAVs hovering throughout the aerial field of $[EX]$ (*i.e.* the air space spanning the length of $[EX]$) may serve as flying base stations hosting a subset of services required by the navigating ground-bound vehicles. Alternatively, these UAVs may serve the objective of extending the coverage of the terrestrial wireless network and, hence, will serve as opportunistic flying relays bridging the connectivity between the vehicles and the ground base station. Here, millimeter wave (mmWave) links may be used to connect the UAV to a ground base station, [33]. UAVs may also communicate with each other using either mmWave and/or Free-Space Optical (FSO) links (*e.g.* [30] and [31]) and, hence, establish an aerial backbone assist network for ground nodes. This is especially feasible since UAVs will have perfect line of sight with each other. One third option is to have these UAVs act as Store-Carry-Forward (SCF) nodes having the ability to receive data from the vehicles and physically carry it to a far away destination or, vice versa, the UAVs may be carrying data from far away sources destined to the isolated vehicles. In either one of the above-enumerated cases, as a UAV hovers throughout $[EX]$'s aerial field and encounters vehicles navigating along this roadway, these latter may opportunistically exploit the services provisioned by this UAV for the limited time interval during which the UAV resides within their respective coverage ranges. Once a UAV departs from the range of a vehicle, the vehicle goes through a disconnection phase awaiting the next UAV's arrival. Throughout its navigation along the considered roadway, one particularly tagged vehicle will experience a sequence of connection times interleaved by disconnection periods; these latter being expectedly dependent on the ground-bound vehicular traffic parameters as well as on the density and speed of the aerial nodes. The fundamental objective of this paper is to capture the dynamics, model and analyze the delay performance of Vehicle-to-UAV (V2U) communications in this particular context.

II. Literature Survey and Novel Contributions

A. Literature Survey

The literature encloses very few seminal work promoting the utility of UAVs in supporting the operability and functionality of ITSs and their underlying vehicular networking infrastructure. For instance, the authors of [18] justifiably argued that automation in next-generation ITSs can be realized through the exploitation of smart and reliable things such as intelligent UAVs. They described the possible ITS applications that may benefit from UAVs together with the problems and challenges this novel communication paradigm brings forward (*e.g.*, energy limitation, dynamic coordination and data routing, security and privacy, and UAV mobility). Also, among these latter challenges is the modeling and characterization of Air-to-Ground (A2G) channels addressed in [20] where it was shown that A2G channel characteristics differ significantly from terrestrial channels. Particularly, A2G channels in scenarios involving communications with Unmanned Aircraft Systems (UASs) differ significantly from those represented by traditional simple A2G channel models (*i.e.*, developed under relatively ideal conditions with tall, well exposed ground stations in wide uncluttered areas with narrowband signalling). In addition to [20], several contemporary surveys (*e.g.*, [22]) and tutorials (*e.g.*, [21]) provide ample information on A2G channel modelling methodologies and related persisting challenges and open issues.

On a different note, In [19], a joint aero-terrestrial cooperative vehicular networking architecture was proposed with the objective of forming an airborne sub-network of multiple UAVs that can assist ground-bound vehicular communications. The work of [23] addressed the advantages of exploiting UAVs for the purpose of data routing and proposed a new UAV-location aware path adjustment extension mechanism to improve the efficiency of data routing in the context of delay-tolerant applications. The authors of [25] investigated how UAVs operating in ad hoc mode can assist the routing process in ground-bound vehicular networks through bridging the gap among communicating entities and, hence, improve the data delivery reliability. The same authors introduced in [26] a novel UAV-assisted reactive and flooding-based routing protocol that incorporated a predictive technique to estimate the expiration time of discovered routing paths. Their reported results showed the significantly improved performance of the UAV-assisted Vehicular Ad Hoc Network (VANET) in terms of the data delivery ratio and delay. This was, indeed, asserted by the study presented in [27]. In [28] an analytical framework was developed for the purpose of determining the best deployment locations that maximize the coverage

areas of UAVs while jointly accounting for the intervention time requirement and UAV battery lifetimes. Parallel to [28], the authors of [29] presented an analytical approach to optimize the hovering altitude of aerial platforms in order to maximize radio coverage on the ground. In contrast the work of [24] revolved around a vehicular sub-network operating under extreme conditions where RSUs became unavailable (*e.g.* destroyed and/or overloaded) causing long segments of a highway to become secluded. In this context, the authors aimed at jointly optimizing the trajectory of deployed UAVs together with the radio resources allocated to them with the objective of maintaining a certain service rate threshold for each serviced vehicle. Also, in a similar context, and in addition to optimizing the UAV trajectories, the authors of [33] aimed at determining the required amount of UAVs needed to meet the requirements of all the navigating vehicles within certain delay bounds.

B. Novel Contributions

The majority of the existing work in the literature (including the above-surveyed prime selection of these publications) revolve around enumerating the benefits of exploiting UAVs to extend the coverage of terrestrial wireless networks (*e.g.*, [18] and [19]) as well as assisting these networks through improving their connectivity (*e.g.*, [27] and [26]) in addition to promoting the performance of the routing processes in terms of reliability and throughput (*e.g.*, [25] and [26]). Nonetheless, the utilization of UAVs for communication purposes are faced with numerous challenges among which is the A2G channel modeling and characterization; a topic surveyed and widely discussed in [20], [21] and [22]. In addition to the above, the placement of UAVs as well as the optimization of their trajectories with the objective of meeting certain service-level requirements has also received significant attention (*e.g.* [24], [28], [33]). However, to the best of our knowledge, an in-depth analysis of the opportunistic V2U data offloading in secluded areas with delay performance insights provided in view of the joint UAV and ground-bound vehicular mobilities has not yet received enough attention. Indeed, this paper revolves around the opportunistic exploitation of flying UAVs as a mean for bringing digital connectivity and services to vehicles navigating in secluded areas where there is no coverage due to the unavailability of communication infrastructure (*i.e.*, disastrous scenarios, overloaded RSUs unable provide services, etc). In such areas, the deployment of additional RSUs may be inefficient as it incurs remarkable capital and operational expenditures (CAPEX/OPEX) due to the considerably elevated installation and maintenance costs of networking infrastructure; let alone their inevitable volatility under extreme conditions. This is not to forget that highways are subject to interleaved low and high vehicular densities as a result of the naturally occurring rush and non-rush hours. Hence, a relatively dense roadside communication networking infrastructure may often appear inefficiently under-utilized. In view of all of the above drawbacks, UAVs present themselves as cost-minimal highly agile, rapid and flexible airborne base stations/access points that contribute to promoting the feasibility of on-demand deployment of aerial networks to serve vehicles in secluded areas. Precisely, instead of having to wait for considerably long periods of time during which a vehicle remains disconnected as it navigates throughout such dark regions, passing by UAVs equipped with computerized modules and wireless communication devices connecting them to backbone networks and wireless base stations may be opportunistically exploited to clear out the data carried by such a vehicle and, hence, reduce the average end-to-end data delivery delay as well as increase the average throughput. Compared to the above-surveyed prime selection of existing work, the distinguishing features of this present paper are:

1) The consideration of a UAV-assisted vehicular sub-networking scenario similar to the one presented in Section I-B and illustrated in Figure 1. In the context of such a scenario, this paper presented an extensive mathematical framework whose objective is to characterize the V2U communication system, capture its dynamics and model the OBU's buffer of a vehicle as a single-server queueing system. The resolution of this latter queueing system allows for the evaluation of the V2U communication performance in terms of essential Quality-of-Service (QoS) metrics and particularly the average System's Response Time (SRT).

2) As opposed to the majority of the earlier-surveyed work that do not account for the realistic UAV and ground-bound vehicular mobilities and their effects on the V2U communication performance, the analytical framework established herein is built on top of a UAV mobility model and a ground-bound vehicular mobility model that are respectively borrowed from [34] and [35] where they were shown to accurately and realistically capture the mobility characteristics (*e.g.*, flow rate, density and speeds) of UAVs and vehicles hovering throughout the aerial field (navigating along) of a straight roadway segment similar to the one illustrated in Figure 1. The UAV and ground-bound vehicle mobility characteristics have a significant impact on the performance of the V2U communication system especially that they constitute an integral component of the residency time of a UAV within a ground-bound vehicle's range (i.e. the time during which the vehicle is connected to the UAV).

3) As opposed to the work of [27] where ground-bound vehicles were considered to have only one packet to transmit to the UAV, in this present work such vehicles are assumed to continuously generate packets following a certain rate.

4) Extensive simulations are conducted with the objective of verifying the validity and accuracy of the derived mathematical formulas and study the performance of the V2U communication system in terms of the achieved SRT in different scenarios subject to UAV availabilities variations and vehicle flow rates.

III. Ground-Bound Vehicular Traffic Model

The considered roadway segment $[EX]$ in Figure 1 is assumed to be an uninterrupted and unidirectional segment with a length of d_{EX} (*meters*) and experiencing Free-Flow ground-bound vehicular traffic with low-to-medium ground-bound vehicular densities. This kind of traffic has been widely employed in the literature (*e.g.*, [34], [36]–[38]). Macroscopic metrics characterizing this type of vehicular traffic flow

dynamics have been theoretically quantified and presented in [34]. A subset of these metrics pertaining to the analysis presented hereafter are as follows.

First, ground-bound vehicles are assumed to arrive following a Poisson process with parameter λ_V $\left(\frac{vehicles}{second}\right)$.[1] It follows that the inter-arrival times of ground-bound vehicles, namely, $\{I_{V,1}, I_{V,2}, I_{V,3}, \cdots\}$, form a sequence of independent and identically distributed (i.i.d.) exponential random variables (r.v.s.) with a mean of λ_V^{-1} (*seconds*). In the sequel, for simplicity, the r.v. I_V will generically denote the inter-arrival time interval between two consecutive ground-bound vehicles entering the considered roadway segment [*EX*] at point *E*.

Second, an arriving vehicle's speed is drawn from a truncated Normal distribution whose probability density function (p.d.f.) is given by:

$$f_V^t(v) = \frac{\zeta}{\sigma_V\sqrt{2\pi}} e^{-\left(\frac{v-\overline{V}}{\sigma_V\sqrt{2}}\right)^2}, \quad v \in [V_{\min}; V_{\max}], \tag{1}$$

where $\overline{V}$ and σ_V respectively denote the mean and standard deviation of the arriving vehicles' speeds in $\left(\frac{meters}{second}\right)$ and $\zeta = 2\left[\text{erf}\left(\frac{V_{\max}-\overline{V}}{\sigma_V\sqrt{2}}\right) - \text{erf}\left(\frac{V_{\min}-\overline{V}}{\sigma_V\sqrt{2}}\right)\right]^{-1}$ is a normalizing constant. The minimum and maximum vehicle speeds are denoted respectively by $V_{\min}$ and $V_{\max}$ and are also expressed in in $\left(\frac{meters}{second}\right)$. Following [34], each arriving vehicle maintains a constant speed throughout its entire navigation period along [*EX*]. Hence, an arbitrary arriving vehicle m with a random speed $V_m = v$ drawn from the distribution whose p.d.f. is given in Equation (1) will reside within [*EX*] for a period $R_{V,m} = d_{EX} \cdot V_m^{-1}$ (*seconds*). Consequently, as proven in [34], the set $\{R_{V,1}R_{V,2}, R_{V,3}, \cdots\}$ constitutes a sequence of i.i.d. r.v.s. with a p.d.f. that is:

$$f_{R_V}(t) = \frac{\zeta}{t^2\sigma_V\sqrt{2\pi}} e^{-\left(\frac{\frac{d_{EX}}{t}-\overline{V}}{\sigma_V\sqrt{2}}\right)^2}, \quad t \in \left[\frac{d_{EX}}{V_{\max}}; \frac{d_{EX}}{V_{\min}}\right]. \tag{2}$$

In the sequel, the r.v. R_V will generically denote an arbitrary ground-bound vehicle's residence time within [*EX*]. Its average and second moment may be numerically computed as:

$$\overline{R_V} = \int_{\frac{d_{EX}}{V_{\max}}}^{\frac{d_{EX}}{V_{\min}}} t \cdot f_{R_V}(t)\mathrm{d}t, \tag{3}$$

$$\overline{R_V^2} = \int_{\frac{d_{EX}}{V_{\max}}}^{\frac{d_{EX}}{V_{\min}}} t^2 \cdot f_{R_V}(t)\mathrm{d}t. \tag{4}$$

IV. UAV Waypoint Mobility Model

The aerial field of the considered roadway segment [*EX*] is defined as the one-dimensional air space spanning the length, d_{EX}, of this segment. The UAV flow rate, λ_U $\left(\frac{UAVs}{second}\right)$, is defined as the average number of UAVs crossing a fixed point within the aerial field of [*EX*] per second. It was shown in [35] that the set $\{I_{U,1}, I_{U,2}, I_{U,3}, \cdots\}$ constitutes a sequence of i.i.d. exponentially distributed inter-arrival times having a mean of λ_U^{-1} (*seconds*).

Now, an arriving UAV, say n, at point E exhibiting a waypoint mobility pattern navigates downstream towards point X at a speed $U_n = u$. As in [35], the per-UAV speeds $\{U_1, U_2, U_3, \cdots\}$ constitute a sequence of i.i.d. uniformly distributed r.v.s. with a p.d.f. $f_U(u)$ and a cumulative distribution function (c.d.f.) $F_U(\nu)$ that are respectively:

$$f_U(u) = \frac{1}{U_{\max} - U_{\min}}, \quad u \in [U_{\min}; U_{\max}] \tag{5}$$

$$F_U(\nu) = \frac{\nu - U_{\min}}{U_{\max} - U_{\min}}, \quad \nu \in [U_{\min}; U_{\max}]. \tag{6}$$

where $U_{\min}$ and $U_{\max}$ respectively denote the minimum and maximum speeds in $\left(\frac{meters}{second}\right)$. Furthermore, it is further assumed hereafter that an arriving UAV, n, to [*EX*]'s aerial field will maintain its speed, U_n, constant all the way throughout its navigation from point E to point X.

V. Modeling and Analysis of V2U Communication

A. Scenario Description

Figure 1 illustrates a general V2U communication scenario. It shows the considered roadway segment [*EX*] populated by a flow of ground-bound vehicles entering the roadway from point E at random times, flowing all the way downstream towards the exit point X. UAVs also enter the aerial field of [*EX*] at random times and hover downstream following a waypoint trajectory above the roadway. UAV speeds are relatively much higher than the speeds of the ground-bound vehicles. As such, any UAV hovering above [*EX*] will enter in contact with an arbitrary vehicle, remain connected to that vehicle for a limited period of time and then exit this latter's communication range. During this time, V2U communication will take place and the vehicle will upload to the UAV data packets stored within its OBU's buffer.[2] This upload process will stop once the OBU's buffer of that vehicle is completely depleted or whenever the UAV departs from that vehicle's range. In this latter case any remaining packets in the vehicle's OBU's buffer will have to further wait until the vehicle encounters another UAV and, hence, resume the upload process. To this end, as mentioned earlier in Section I-B, a packet-level observation of the vehicle's OBU's buffer will reveal that a packet occupying that buffer's Head-of-Line (HoL) position will be successfully cleared out with a probability of P_c; this being the probability that the vehicle is in contact with a UAV. Otherwise, with a probability of $1-P_c$, the waiting time of this packet will be further extended until contact is established with a subsequent UAV allowing its clearance. Assuming that the vehicle will generate packets at random, the vehicle's OBU's buffer may be abstracted as a single-server queueing system with the HoL position of the queue being the service position. This queueing system is illustrated in Figure 3. In what follows, the characterizing

[1] The roadway segment may comprise a number of N lanes. Similar to [39], the vehicle arrivals to lane i ($1 \leq i \leq N$) may be assumed to follow a Poisson sub-process with parameter $\lambda_V^{(i)}$. Consequently, the aggregate vehicle arrival process to the entire roadway segment is a Poisson process with parameter $\lambda_V = \sum_{i=1}^{N} \lambda_V^{(i)}$.

[2] Vehicle OBUs are assumed to be quite large (*e.g.*, 1TB and beyond). The moderate packet generation rate will never lead to the exhaustion of such a large buffer before a V2U contact arises. As such, the OBUs' buffers emulate infinite buffers.

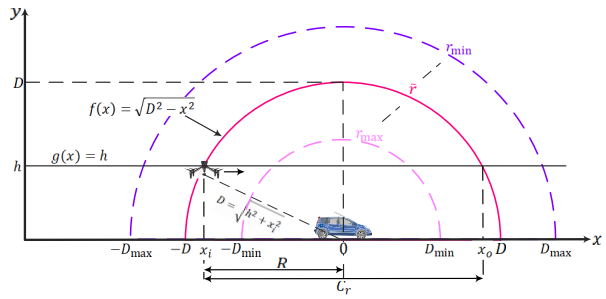

Fig. 2. Relationship between the achieved bit rate and V2U coverage distance.

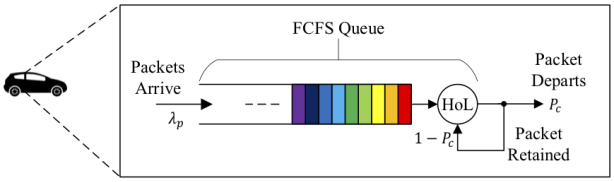

Fig. 3. Queueing system representation of a vehicle's OBU's buffer.

parameters of this queueing system necessary to study its dynamics will be formulated.

B. Air-to-Ground Channel and V2U Coverage Range

In the context of the scenario illustrated in Figure 1, UAVs fly right on top of the considered highway segment. Hence, they establish with ground-bound vehicles communication links that are assumed to be dominated by direct Line-of-Sight (LoS). In addition, the communication channel may be assumed to be ideal where signals are only subject to path losses due to their propagation over distances that separate the transmitting (Tx) and receiving (Rx) nodes. This is especially true since the considered highway segment is located in a secluded area with minimum structural obstacles (*e.g.*, buildings, bridges, tunnels, etc). Accordingly, the established communication links between UAVs and ground-bound vehicles experience quite negligible multi-path effect.

In light of the above and without loss of generality (w.l.o.g.), the achieved bit rate, r in bits per second (bps), between the ground-bound vehicle and the UAV is $r = B\log_2\left(1 + S \cdot N^{-1}\right)$, where B denotes the channel bandwidth and $S \cdot N^{-1} = P_t D^{-\alpha} N_0^{-1}$ denotes the signal-to-noise ratio with P_t being the vehicle's transmission power, D being the distance separating the Tx (*i.e.*, the vehicle) from the Rx (*i.e.*, the UAV) as illustrated in Figure 2, α being the path-loss exponent and N_0 being the noise spectral density. It follows that the normalized bit rate is:

$$\widetilde{r} = \log_2\left(1 + P_t D^{-\alpha} N_0^{-1}\right). \tag{7}$$

Here note that, in order for a wireless communication link to be established between a Tx and a Rx, the bit rate $\widetilde{r}$ is required to be greater than or equal to a certain minimum threshold $r_{\min}$. The maximum achievable bit rate is also denoted by $r_{\max}$. As such $r_{\min} \leq r \leq r_{\max}$. To each value of the achievable bit rate corresponds a value for the Tx-Rx distance (*i.e.*, the distance D in Figure 2). Indeed, the bit rate increases as the Tx-to-Rx distance decreases. In Figure 2, the distance $D_{\min}$ corresponds to the maximum feasible distance required to achieve a bit rate of $r_{\max}$ while $D_{\max}$ corresponds to the maximum feasible distance, beyond which no wireless communication link between the Tx and the Rx can be established. Accordingly, a link between the Tx and Rx can be established only whenever the distance D in Equation (7) falls within the range $[D_{\min}; D_{\max}]$ where:

$$D_{\min} = \left[P_t N_0^{-1}\left(2^{r_{\max}} - 1\right)^{-1}\right]^{\frac{1}{\alpha}}, \tag{8}$$

$$D_{\max} = \left[P_t N_0^{-1}\left(2^{r_{\min}} - 1\right)^{-1}\right]^{\frac{1}{\alpha}}. \tag{9}$$

At this point, note that safety regulations, the UAV type/capability, the UAV deployment area and possibly other factors constrain the minimum and maximum heights (respectively denoted herein by $h_{\min}$ and $h_{\max}$) at which UAVs are allowed to fly such that they do not incur any safety/security threats. Determining the values of $h_{\min}$ and $h_{\max}$ is outside the scope of this present work. However, it is important to mention that if $h_{\max} > D_{\max}$, no V2U communication link can be established. Else, if $h_{\max} < D_{\max}$, then the maximum attainable height will be $h_{\max}$ irrespective of the V2U communication feasibility beyond that height. Ultimately, at $h_{\max}$, the achievable data rate lower limit will be $r_{\lim} = \log_2\left(1 + P_t h_{\max}^{-\alpha} N_0^{-1}\right)$ and is larger than $r_{\min}$ achieved at $D_{\max}$. In the sequel, all UAVs are assumed to fly within the allowable safe flight zone at a height h such that $h_{\min} \leq h \leq h_{\max}$.

Now, if the vehicle's achievable bit rate is $\widetilde{r}$ as computed in Equation (7) and such that $r_{\lim} \leq \widetilde{r} \leq r_{\max}$, the three-dimensional (3D) coverage range of the vehicle is the top half-sphere having a radius that is equal to D (meters) where $h_{\min} \leq D \leq h_{\max}$. Projecting this coverage range onto a two-dimentional (2D) plane, the coverage range of the vehicle becomes the top half-circle of radius D. The equation of this top half-circle is $f(x) = \sqrt{D^2 - x^2}$ ($x \in [-D; D]$). Next, consider a UAV hovering on top of the vehicle's trajectory at a height of h as illustrated in Figure 2 such that $h_{\min} \leq h \leq D$. In view of the earlier-presented UAV waypoint mobility pattern in Section IV, this UAV will constantly navigate at the height h until it goes out of the vehicle's coverage range. Here, interest lies in computing the V2U coverage distance, travelled by the UAV from the instant it enters the vehicle's coverage range until the instant it leaves this vehicle's range. This coverage distance is denoted by C_r. To compute C_r, it is required to determine the abscissas of the entry and exit points, respectively, x_i and x_o. This is equivalent to finding the abscissas of the intersection points between the top-half circle of equation $f(x)$ given above and the horizontal line having an equation $g(x) = h$. These are easily shown to be $x_i = -\sqrt{D^2 - h^2}$ and $x_o = \sqrt{D^2 - h^2}$. Here, the V2U coverage distance is given by:

$$C_r(h) = x_o - x_i = 2\sqrt{D^2 - h^2}, \quad h \in [h_{\min}; D]. \tag{10}$$

Observe from Equation (10) that whenever the UAV is hovering at a maximum distance of $h > D$, there will be no intersection between the UAV's aerial path and the considered

vehicle's coverage range. Hence, no wireless link may be established between the vehicle and the UAV.

Remark: In the sequel, it will be assumed that the vehicle will transmit data at the minimum possible rate r_{lim}. Obviously, at a higher rate, the V2U communication system's performance will further improve. This is especially true since, given a certain fixed period of time, the vehicle, at a higher rate, will be able to clear out more packets from its OBU's buffer. In addition, to work around the analytical complexity and promote the tractability of the below analysis, it will be assumed that all arriving UAVs will be hovering at a fixed distance of h. Thus, the V2U coverage distance will become a fixed constant that will be denoted by $C_r = 2R$ where R, as shown in Figure 2 denotes half of this distance.

C. Packet Arrivals

Any arriving vehicle is assumed to generate packets according to a Poisson process with a parameter $\lambda_P \left(\frac{packets}{second}\right)$. As such, the packet inter-arrival time is exponentially distributed with a mean of λ_P^{-1} (*seconds*). The generated packets will be stored in the generating vehicle's OBU's buffer and will be served following a First-Come-First-Serve (FCFS) service discipline.

D. V2U Connection/Disconnection Process Characterization

This subsection is dedicated to derive a theoretical expression for the V2U contact probability, which was referred to as P_c in Section V-A as well as to theoretically quantify: *i*) the distribution of the number, N_C, of UAVs that an arbitrary vehicle encounters and connects to throughout its navigation period along the considered roadway segment [*EX*] and its average, $\overline{N_C}$, as well as *ii*) the distribution of, R_{UV}, being the V2U per-contact duration together with its average $\overline{R_{UV}}$.

1) V2U Contact Probability: W.l.o.g., consider the arrival of an arbitrary vehicle with a random speed of V drawn according to the distribution whose p.d.f. is given in (1). Since V remains constant throughout the vehicle's navigation along [*EX*], that vehicle's overall residence time within [*EX*] is, therefore, $R_V = d_{EX}V^{-1}$ (*seconds*). Now, throughout the vehicle's navigation along [*EX*], this latter experiences the arrival of UAVs at random distinct times t_1, t_2, t_3, ..., t_n where t_1 and t_n respectively denote the arrival time of the first UAV that arrives after the considered vehicle enters the roadway at point E as well as the arrival time of the last UAV that arrives before the considered vehicle departs from [*EX*] at point X. At this point, recall from Section III that UAV arrivals follow a Poisson process with a parameter $\lambda_U \left(\frac{UAVs}{second}\right)$. Hence, given the time interval R_V, the arrival times of these UAVs are uniformly distributed along this interval, [41]. As such, given that the vehicle's speed is constant, the location L_V of the vehicle within [*EX*] is a uniformly distributed r.v. with a p.d.f. and c.d.f. that are given by:

$$f_{L_V}(l) = \frac{1}{d_{EX}}, \quad l \in [0; d_{EX}], \tag{11}$$

$$F_{L_V}(\lambda) = \int_0^{\lambda} f_{L_V}(l)\mathrm{d}l = \frac{\lambda}{d_{EX}}, \quad \lambda \in [0; d_{EX}]. \tag{12}$$

Now, consider a randomly arriving UAV at an arbitrary time t_0. This UAV has a speed of U drawn following a distribution whose p.d.f. is given in (5). Also recall from Section IV that U remains constant throughout the UAV's entire hovering duration over [*EX*]. At the time of arrival of the UAV, the vehicle is assumed to be found at a location $L_V = l$ somewhere within [*EX*]. At this point, interest lies in determining the necessary condition that needs to be satisfied in order for the UAV that has just arrived to be able to connect with the vehicle prior to this latter's departure from [*EX*]. In this regard, at time t_0, on one hand, the residual residence time of the vehicle within [*EX*] is $R_V^{\text{res}} = (d_{EX} - L_V) \cdot V^{-1}$. On the other hand, the time required for the arriving UAV to reach and connect with the vehicle is $T_c = (L_V - R) \cdot (U-V)^{-1}$. It follows that the sought condition for the arriving UAV to connect to the vehicle is:

$$\begin{aligned} T_c < R_V^{\text{res}} &\Rightarrow \frac{L_V - R}{U - V} < \frac{d_{EX} - L_V}{V} \\ &\Rightarrow L_V < d_{EX}\left(1 - \frac{V}{U}\right) + R\left(\frac{V}{U}\right). \end{aligned} \tag{13}$$

As such, the conditional probability of V2U connection can be derived as follows:

$$\begin{aligned} &P_c(u, v) \\ &= \Pr\left[L_V < d_{EX}\left(1 - \frac{V}{U}\right) + R\left(\frac{V}{U}\right) \middle| U = u, V = v\right] \\ &= 1 - \left(1 - \frac{R}{d_{EX}}\right)\frac{v}{u}. \end{aligned} \tag{14}$$

It follows that the unconditional probability of V2U connection can be derived as:

$$\begin{aligned} P_c &= \int_{U_{\min}}^{U_{\max}} \int_{V_{\min}}^{V_{\max}} \left[1 - \left(1 - \frac{R}{d_{EX}}\right)\frac{v}{u}\right] f_V^t(v) f_U(u)\mathrm{d}v\mathrm{d}u \\ &= 1 - \frac{\overline{V} \cdot \ln\left(U_{\max} \cdot U_{\min}^{-1}\right)}{U_{\max} - U_{\min}}\left(1 - \frac{R}{d_{EX}}\right). \end{aligned} \tag{15}$$

2) Number of Distinct V2U Contacts: Throughout the navigation period R_V of the above-considered tagged vehicle along [*EX*], assume that this latter witnesses the arrival of $N_A = n_a$ UAVs. In view of the Poisson UAV arrivals with parameter λ_U and fixing $t \leq R_V \leq t + \mathrm{d}t$, the conditional probability mass function (p.m.f.) of N_A can be derived as:

$$\begin{aligned} f_{N_A|R_V}(n_a) &= \Pr\left[N_A = n_a \middle| \mathrm{d}t \leq R_V \leq t + \mathrm{d}t\right] \\ &= \frac{(\lambda_U t)^{n_a}}{n_a!} \cdot e^{-\lambda_U t}, \end{aligned} \tag{16}$$

where $n_a \geq 0$. Hence, the unconditional p.m.f. and c.d.f. of N_A are:

$$f_{N_A}(n_a) = \int_{\frac{d_{EX}}{V_{\max}}}^{\frac{d_{EX}}{V_{\min}}} \frac{(\lambda_U t)^{n_a}}{n_a!} \cdot e^{-\lambda_U t} \cdot f_{R_V}(t)\mathrm{d}t \tag{17}$$

$$F_{N_A}(n) = \Pr[N_A \leq n] = \sum_{n_a=0}^{n} f_{N_A}(n_a), \tag{18}$$

where $f_{R_V}(t)$ is given in (2). Now, as the considered tagged vehicle navigates along [*EX*], it will, with a probability of P_c

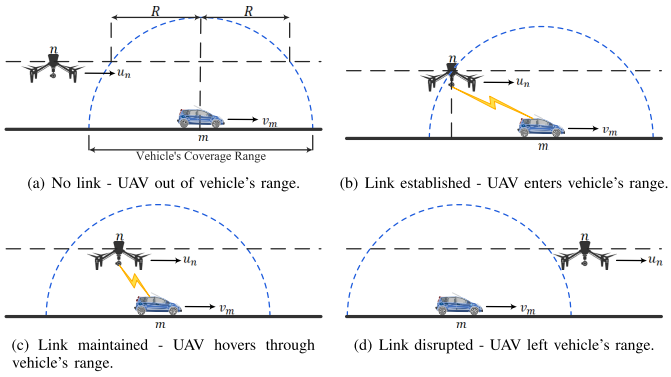

(a) No link - UAV out of vehicle's range. (b) Link established - UAV enters vehicle's range.

(c) Link maintained - UAV hovers through vehicle's range. (d) Link disrupted - UAV left vehicle's range.

Fig. 4. V2U contact establishment and disruption dynamics.

(as derived in Section V-C.1), encounter an arriving UAV. Otherwise, with a probability of $1-P_c$, this vehicle will not be able to connect with that arriving UAV. Thus, given $N_A = n_a$, the conditional p.m.f. of N_C is $f_{N_C|N_A}(n_c) = \Pr\left[N_C = n_c \middle| N_A = n_a\right] = \binom{n_a}{n_c} P_c^{n_c}(1-P_c)^{n_a-n_c}$ As such, for $0 < n_c \leq n_a$, the unconditional p.m.f. and c.d.f. of $N_C = n_c$ can be derived as $f_{N_C}(n_c) = \Pr[N_C = n_c] = \sum_{\forall n_a} f_{N_C|N_A}(n_c) \cdot f_{N_A}(n_a)$ and $F_{N_C}(n) = \Pr[N_C \leq n] = \sum_{n_c=0}^{n} f_{N_C}(n)$. Unfortunately, none of $f_{N_A}(n_a)$, $f_{N_C}(n_c)$, $F_{N_A}(n)$ and $F_{N_C}(n)$ has a closed-form expressions. They will be evaluated numerically. Let $\overline{N_C}$ and $\overline{N_C^2}$ respectively denote the mean and second moment of N_C such that:

$$\overline{N_C} = E[N_C] = \sum_{\forall n_c} n_c \cdot f_{N_C}(n_c), \tag{19}$$

$$\overline{N_C^2} = E[N_C^2] = \sum_{\forall n_c} n_c^2 \cdot f_{N_C}(n_c) - \overline{N_C}^2. \tag{20}$$

3) V2U Per-Contact Duration: Consider the above-mentioned tagged vehicle m whose speed is $V_c = v_m$ and is navigating along $[EX]$ as shown in Figure 4. Also, consider a tagged UAV n whose speed is $U_c = u_n$, which, following its arrival to $[EX]$, hovered downstream towards vehicle m and, eventually, with a probability of P_c, was able to connect to it. Here, it is worthwhile mentioning that the above-mentioned vehicle and UAV speeds where denoted with variables V_c and U_c as they represent the speeds of a vehicle and a UAV that got connected. These speeds have different distributions from the typical vehicle and UAV speeds, respectively V and U that were defined earlier in Sections III and IV. The distributions of V_c and U_c are derived hereafter.

Now, define the V2U per-contact duration, denoted herein by R_{V2U}, to be the time interval during which UAV n resided within the communication range of vehicle m. Here, observe that the overall communication range of both the vehicle and the UAV is $C_r = 2R$ (as shown in Figure 4(a)) where, R, as mentioned in Section V-A, is the radius of that range. Figures 4(b) and 4(c) illustrate the contact establishment and maintenance phases until the contact is disrupted upon the departure of the UAV from the vehicle's range as shown in Figure 4(d). Consequently, as both the UAV and the vehicle are in motion at different speeds, then $R_{V2U} = C_r \cdot \Delta S^{-1}$ where $\Delta S = U_c - V_c$ is the relative speed of motion corresponding to a connected pair of nodes (*i.e.* one UAV, say UAV n, and one vehicle, say vehicle m).[3] Clearly, with a probability of $1-P_c$, the considered UAV and vehicle will not enter in contact with each other and, therefore, in this latter case, $R_{V2U} = 0$. Grouping those two cases together:

$$R_{V2U} = \begin{cases} 0, & \text{with a probability } 1-P_c \\ \dfrac{C_r}{U_c - V_c}, & \text{with a probability } P_c \end{cases} \tag{21}$$

Obviously, here, R_{V2U} is a r.v. whose value is dependent on P_c and the relative speed ΔS. Consequently, if the p.d.f. of R_{V2U} is denoted by $f_{R_{V2U}}(t) = \Pr[t \leq R_{V2U} \leq t + \mathrm{d}t]$, then it is clear from the above that $f_{R_{V2U}}(0) = 1 - P_c$. Now, for $t \neq 0$, the first step in deriving an expression for $f_{R_{V2U}}(t)$ in this case will be to derive the p.d.f. of ΔS, which is denoted herein by $f_{\Delta S}(\delta)$. In view of the above definition of ΔS, this r.v. is equivalent to the difference between two r.v.s., one of which is U_c that is drawn from the range $[U_{\min}; U_{\max}]$ and the other is V_c that, in turn, is defined over the range $[V_{\min}; V_{\max}]$. Hence, in order to derive $f_{\Delta S}(\delta)$, it is necessary to derive the p.d.f.s of U_c and V_c, respectively $f_{U_c}(u)$ and $f_{V_c}(v)$. Define:

$$P_c(u) = \int_{V_{\min}}^{V_{\max}} P_c(u,v) f_V^t(v) \mathrm{d}v = 1 - F_{L_V}^c(R) \overline{V} u^{-1}, \tag{22}$$

$$\begin{aligned} P_c(v) &= \int_{U_{\min}}^{U_{\max}} P_c(u,v) f_U(u) \mathrm{d}u \\ &= 1 - \ln\left(\frac{U_{\max}}{U_{\min}}\right)\left(\frac{F_{L_V}^c(R)}{U_{\max} - U_{\min}}\right) v, \end{aligned} \tag{23}$$

where $F_{L_V}^c(R) = 1 - F_{L_V}(\lambda)|_{\lambda=R}$ is the complementary c.d.f. (c.c.d.f.) of L_V with $F_{L_V}(\lambda)$ as given in (12) and $P_c(u,v)$ is given in (14). At this point, it becomes easy to show that:

$$f_{U_c}(u) = \frac{f_U(u) \cdot P_c(u)}{P_c}, \quad u \in [U_{\min}; U_{\max}], \tag{24}$$

$$f_{V_c}(v) = \frac{f_V^t(v) \cdot P_c(v)}{P_c}, \quad v \in [V_{\min}; V_{\max}]. \tag{25}$$

At this point, ΔS may be re-defined as $\Delta S = U_c + W_c$ where $W = -V_c$. Consequently, the p.d.f. of ΔS will become equivalent to the convolution of the p.d.f. of U_c with the p.d.f. of W_c. Here, it is very easy to prove that the p.d.f. of W_c, denoted by $f_{W_c}(w) = f_{V_c}(-w)$ for $w \in [-V_{\max}; -V_{\min}]$. It follows that the p.d.f. of ΔS can be derived as:

$$f_{\Delta S}(\delta) = f_{U_c}(u) * f_{W_c}(w) = \int_{-\infty}^{+\infty} f_{U_c}(u) \cdot f_{W_c}(\delta - u) \mathrm{d}\delta, \tag{26}$$

where $\delta \in [U_{\min} - V_{\max}; U_{\max} - V_{\min}]$. Owing to its complexity as well as space limitation, the derivation of a closed-form expression of $f_{\Delta S}(\delta)$ is omitted and this latter p.d.f. will be evaluated numerically where needed. Now, define $F_{\Delta S}(s) = \Pr[\Delta S \leq s]$ to be the c.d.f. of ΔS where $s \in [U_{\min} - V_{\max}; U_{\max} - V_{\min}]$. $F_{\Delta S}(s)$ is given by:

$$F_{\Delta S}(s) = \int_{U_{\min} - V_{\max}}^{s} f_{\Delta S}(\delta) \mathrm{d}\delta. \tag{27}$$

[3]Typically, highways may be bidirectional. Hence, in the case where the UAV and the vehicle are moving in opposite directions, the relative speed is computed as $\Delta S = U_c + V_c$.

Note that $F_{\Delta S}(\delta)$ will also be computed numerically. Armed with the c.d.f. of ΔS, now, in the case where $R_{V2U} = C_r \cdot \Delta S^{-1}$, the c.d.f. of this r.v. can be derived as follows:

$$F_{R_{V2U}}(\tau) = \Pr\left[R_{V2U} \leq \tau\right] = \Pr\left[\frac{C_r}{\Delta S} \leq \tau\right] = \Pr\left[\Delta S \geq \frac{C_r}{\tau}\right] = 1 - F_{\Delta S}\left(\frac{C_r}{\tau}\right). \quad (28)$$

Consequently, in that case, the p.d.f. of R_{V2U} is:

$$f_{R_{V2U}}(t) = \frac{\mathrm{d}}{\mathrm{d}\tau} F_{R_{V2U}}(\tau)\bigg|_{\tau=t} = \frac{C_r}{\tau^2} f_{\Delta S}\left(\frac{C_r}{\tau}\right)\bigg|_{\tau=t}, \quad (29)$$

for $C_r \cdot \Delta S_{\max}^{-1} \leq t \leq C_r \cdot \Delta S_{\min}^{-1}$ with $\Delta S_{\max} = U_{\max} - V_{\min}$ and $\Delta S_{\min} = U_{\min} - V_{\max}$. At this level, it must not be forgotten that in the case where $t = 0$, $f_{R_{V2U}}(t) = 1 - P_c$. Hence, grouping the two cases together leads to having:

$$f_{R_{V2U}}(t) = \begin{cases} 1 - P_c, & t = 0 \\ P_c\left[\dfrac{C_r}{t^2} f_{\Delta S}\left(\dfrac{C_r}{t}\right)\right], & \dfrac{C_r}{\Delta S_{\max}} \leq t \leq \dfrac{C_r}{\Delta S_{\min}} \end{cases} \quad (30)$$

As such, the average V2U per-contact duration, $\overline{R_{V2U}}$, is:

$$\overline{R_{V2U}} = E\left[R_{V2U}\right] = P_c \int_{\frac{C_r}{U_{\min} - V_{\max}}}^{\frac{C_r}{U_{\max} - V_{\min}}} t \cdot f_{R_{V2U}}(t)\mathrm{d}t. \quad (31)$$

The variance of R_{V2U}, $\sigma^2_{R_{V2U}}$, is numerically computed as:

$$\overline{R^2_{V2U}} = E\left[R^2_{V2U}\right] = P_c \int_{\frac{C_r}{U_{\min} - V_{\max}}}^{\frac{C_r}{U_{\max} - V_{\min}}} t^2 \cdot f_{R_{V2U}}(t)\mathrm{d}t. \quad (32)$$

4) Overall Average V2U Connection and Disconnection Durations: From the time it arrives to [*EX*] and throughout its navigation along this entire roadway, the previously considered tagged vehicle may encounter several UAVs. Hence, it may, as shown in Figure 5, experience a sequence of interleaved connection and disconnection times referred herein as ON (*i.e.* connected) and OFF (*i.e.* disconnected) times until it, eventually, departs from [*EX*]. The characterization of the average overall V2U connection duration is derived first.

Let T_C be an r.v. representing the overall time duration during which the considered tagged vehicle happens to be in contact with passing by UAVs throughout its residence time R_V within [*EX*]. Recall from Section V-C.2 that the number of UAVs the vehicle may encounter throughout R_V is $N_C = n_c$ where $0 \leq n_c \leq N_A$ with N_A being an r.v. representing the number of UAVs that may arrive to [*EX*] during R_V. Hence, to start with, set up a first condition that $R_V = t$. This, in other words, is equivalent to limiting N_A to a certain number, say n_a (*i.e.* $N_A = n_a$). Hence, in this case, the value n_c will vary in the range $[0; n_a]$. Let $R^{(i)}_{V2U}$ denote the contact duration between UAV i ($1 \leq i \leq n_c$) and the tagged vehicle. Also, let $T_C(n_c)$ represent a version of T_C that is conditional on the fact that $N_C = n_c$. It is expressed as:

$$T_C(n_c) = \begin{cases} 0, & n_c = 0 \\ \displaystyle\sum_{i=1}^{n_c} R^{(i)}_{V2U}, & 0 < n_c \leq n_a \end{cases} \quad (33)$$

Now, recall that $\{R^{(i)}_{V2U} | 1 < i \leq n_c\}$ constitutes a sequence of i.i.d. V2U per-contact durations drawn from a common distribution whose p.d.f is given in (30) and average is $\overline{R_{V2U}}$, which is given in (31). Hence, the average of $T_C(n_c)$ is:

$$\overline{T_C(n_c)} = E\left[T_C(n_c)\right] = n_c \cdot \overline{R_{V2U}}, \quad n_c \in [0; n_a]. \quad (34)$$

Thus, the unconditional average overall V2U connection duration can be easily proven to be:

$$\overline{T_C} = \overline{N_C} \cdot \overline{R_{V2U}} \quad (35)$$

where $\overline{N_C}$ is given in (19). Now, as derived in Equation (33), T_C is the sum of a random number of N_C identical and i.i.d. R_{V2U} random variables whose statistical characteristics (*i.e.* c.d.f., p.d.f., mean and variance) have been derived earlier in Section V-C.3. Consequently, the second moment of T_C is:

$$\overline{T^2_C} = E\left[T^2_C\right] = E\left[E\left[T^2_C \middle| N_C\right]\right] = \overline{N^2_C} \cdot \overline{R^2_{V2U}}, \quad (36)$$

where $\overline{N^2_C}$ and $\overline{R^2_{V2U}}$ have been respectively derived in Equations (20) and (32). At this level, it becomes possible to characterize the overall disconnection time, denoted herein by T_D, which represents the overall time period during which the vehicle is disconnected. The mean of T_D is:

$$\overline{T_D} = \overline{R_V} - \overline{T_C}, \quad (37)$$

where $\overline{R_V}$ is the average vehicle residence time within [*EX*] and is given in (3). In computing the variance of T_D, it is important to keep in mind that R_V and T_C are not independent random variables. Indeed, the root of the correlation between R_V and T_C goes back to the correlation between T_C and N_C. Here, recall from Section V-C.2 that $N_C \leq N_A$ where N_A is the number of UAVs arriving during the navigation time R_V of a certain tagged vehicle. Consequently, in view of this correlation, the variance of T_D has to be computed as follows:

$$\sigma^2_{T_D} = \sigma^2_{R_V} + \sigma^2_{T_C} - 2\sigma_{R_V,T_C}, \quad (38)$$

where $\overline{R^2_V}$ and $\overline{T^2_C}$ are respectively given in Equations (4) and (36) while $\sigma_{R_V,T_C} = E\left[\left(R_V - \overline{R_V}\right)\left(T_C - \overline{T_C}\right)\right]$ can be easily computed numerically. It follows that the second moment of T_D is $\overline{T^2_D} = \sigma^2_{T_D} + \overline{T_D}^2$.

Now, denote by T^{pc}_D the per-contact vehicle disconnection time; that is, the time duration, which is delimited by: *a*) the time instant when a UAV that, earlier, got connected to the vehicle, now, disconnects from this latter as it leaves its communication range, and, *b*) the time instant when a subsequent new UAV connects to that same vehicle as it enters its communication range. The average and second moment of T^{pc}_D are respectively denoted by $\overline{T^{pc}_D}$ and $\overline{(T^{pc}_D)^2}$. Knowing that the considered vehicle encounters an average of $\overline{N_C}$ UAVs (*i.e.* experiences on average $\overline{N_C}$ connection durations), therefore, it will also experience $\overline{N_C}$ disconnection durations. As such:

$$\overline{T^{pc}_D} = \overline{T_D} \cdot \overline{N_C}^{-1}, \quad (39)$$

$$\overline{(T^{pc}_D)^2} = E\left[T_D \cdot N_C^{-1}\right]. \quad (40)$$

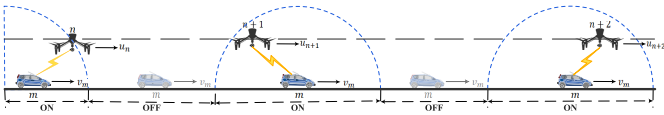

Fig. 5. Interleaved connection/disconnection times for an arbitrary vehicle m.

E. Average and Second Moment of a Packet's Service Time

In view of the queueing system representation illustrated in Figure 3, the service time, S, of a certain tagged packet P consists of the amount of time that P will spend occupying the HoL position of its carrying vehicle's OBU's buffer from the time instant P reaches that position until the time it gets successfully cleared out to an in-range UAV. In this present work, the vehicle is assumed to be subject to a heavy data traffic load (*i.e.* it always has a packet to transmit when connected). Hence, as long as the considered tagged vehicle is connected (*i.e.* with a probability of P_c given by Equation (15)) to a UAV it keeps on transmitting packets to that UAV in a back to back manner. Under such conditions, a packet that arrives to the HoL position of that vehicle's OBU's buffer is immediately cleared out (*i.e.* transmitted to the UAV) and, thus, such a packet has a service time of $S = \tau$ where $\tau = \frac{L_P}{\widetilde{r}}$ is the packet's transmission delay with L_p being the packet size in (*bits*) and $\widetilde{r}$ being the transmission rate in (*Mbps*) as defined in Section V-B. Alternatively, with a probability of $1 - P_c$, the vehicle finds itself disconnected. Under such circumstances, a packet occupying the HoL position of that vehicle's OBU's buffer is retained until the vehicle goes back in contact with another UAV. The amount of time that such a packet will have to wait is nothing but the vehicle's per-contact disconnection time, T_D^{pc}, which was defined herein in Section V-C.4 and whose mean and second moment are given respectively by Equations (39) and (40). This can be explained as follows. Without loss of generality, assume that a certain tagged vehicle m got connected to a certain UAV n at a certain time t_c. With packets already queueing within its OBU's buffer, the vehicle immediately starts clearing them out one after the other until, at time t_{dc}, UAV n goes out of vehicle m's coverage range and, therefore, vehicle m gets disconnected. Assume that the last packet vehicle m transmitted to UAV n was packet P_k. Accordingly, the next packet P_{k+1}, has reached the HoL position of the vehicle's OBU's buffer and will be bound to wait until the subsequent UAV $n+1$ arrives and connects to vehicle m. Consequently, the amount of time packet P_{k+1} will have to wait is exactly equal to T_D^{pc}. It follows that, with a probability of $1 - P_c$, the packet's service time will be $S = \tau + T_D^{pc}$. Combining the above two cases leads to having:

$$\begin{aligned} S &= P_c \cdot \tau + (1 - P_c) \cdot (\tau + T_D^{pc}) \\ &= \tau + (1 - P_c) \cdot T_D^{pc} \approx (1 - P_c) \cdot T_D^{pc}. \end{aligned} \tag{41}$$

Here, observe that, in Equation (41), packet service time has been approximated by $(1 - P_c) \cdot T_D^{pc}$ where the transmission delay has been discarded. The rationale behind this is as follows. Under the IEEE $802.11p$ protocol used for communication in the context of the V2U communication scenario presented herein, the Maximum Transmission Unit (MTU) size is equal to 1500 bytes. In the case where the adopted bit rate is as low as 1 Mbps, the required amount of time to transmit a maximum sized packet is equal to $\tau = 12$ milliseconds (ms), which is way much smaller than the queueing delay; let alone the amount of time a packet waits at the Head-of-Line (HoL) of the vehicle's OBU's buffer until that vehicle enters in contact with a UAV and, hence, it gets transmitted. At this point, note that, if smaller packet sizes are used and/or the transmission rate is increased the resulting value of τ will get even smaller and its contribution to the overall system's performance will become negligible. To this end, the average and second moment of S, respectively $\overline{S}$ and $\overline{S^2}$, are:

$$\overline{S} = (1 - P_c) \cdot \overline{T_D^{pc}}; \quad \overline{S^2} = (1 - P_c)^2 \overline{(T_D^{pc})^2}. \tag{42}$$

F. Vehicle OBU's Buffer Queuing Model Resolution

Armed with the fact that packet arrivals follow a Poisson process with parameter λ_P (refer to Section V-B) and the packet service time characteristics (refer to Section V-D), a certain tagged vehicle's OBU's buffer illustrated in Figure 3 can be represented as an *M*/*G*/1 queueing system whose characteristics have been widely studied in the literature (*e.g.* [41]). In this work, interest lies in characterizing the average System's Response Time (SRT) (*i.e.* the average waiting time of packets in the vehicle's OBU's buffer), which is denoted herein by $\overline{Q_D}$. From [41]:

$$\overline{Q_D} = \overline{S} + \frac{\rho \overline{S}(1 + C_v^2)}{2(1 - \rho)}, \tag{43}$$

where $C_v^2 = \sigma_S^2 \cdot \overline{S}^{-2}$ is the squared coefficient of variation of S with $\sigma_S^2 = \overline{S^2} - \overline{S}^2$ being the variance of this latter and $\rho = \lambda_P \cdot \overline{S}$ is the vehicle's data packet load.

VI. Simulations and Numerical Analysis

A. Simulation Setup

In order to verify and assert the validity, correctness and accuracy of the expressions derived in Section V, realistic ground-bound vehicular mobility traces were obtained using the Simulation of Urban MObility (SUMO), [42]. In addition, the following parameters were considered: *a*) $\lambda_V \in [0.1; 0.277]$ (Veh/s), *b*) $\lambda_U \in [0.01; 0.1]$ (UAV/s), *c*) $d_{SD} = 10$ (Km), *d*) $R = 500$ (m), *e*) fixed packet sizes of 1500 (bytes), *f*) $\lambda_P \in [0.1; 1]$ (Pkt/s), *g*) $[V_{\min}; V_{\max}] = [10; 50]$ (m/s) and *g*) $[U_{\min}; U_{\max}] = [100; 150]$ (m/s). The above-mentioned traces and parameters were fed as inputs into a custom-built PYTHON-based discrete-event simulator. All results reported herein were averaged out over ten runs of the simulator with each run spanning a time interval that is sufficiently large to allow for the arrival and departure of 10^6 ground-bound vehicles. Upon the end of each simulation run, the overall number of packets generated will be of the order of 10^9 packets. Statistics will be collected from vehicles and packets to realize a confidence interval of 95%.

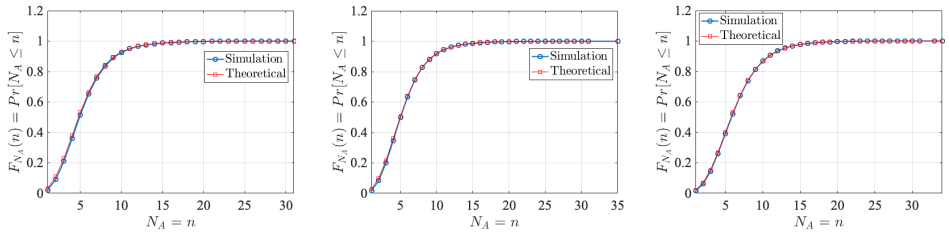

(a) $\lambda_V = 0.1$ (Veh/s) (b) $\lambda_V = 0.15$ (Veh/s) (c) $\lambda_V = 0.25$ (Veh/s)

Fig. 6. Simulated vs. theoretical c.d.f. of N_A for different λ_V.

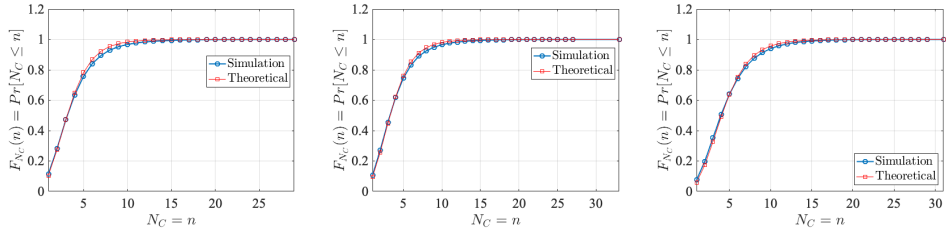

(a) $\lambda_V = 0.1$ (Veh/s) (b) $\lambda_V = 0.15$ (Veh/s) (c) $\lambda_V = 0.25$ (Veh/s)

Fig. 7. Simulated vs. theoretical c.d.f. of N_C for different λ_V.

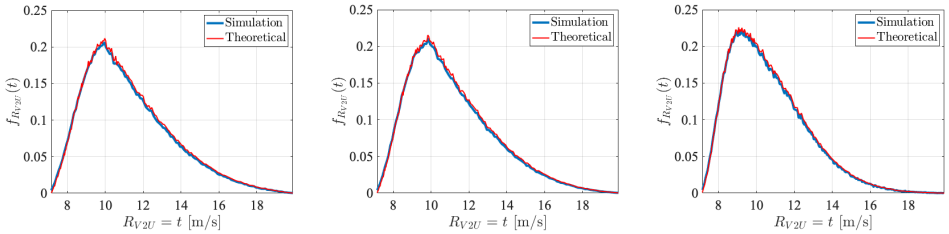

(a) $\lambda_V = 0.1$ (Veh/s) (b) $\lambda_V = 0.15$ (Veh/s) (c) $\lambda_V = 0.25$ (Veh/s)

Fig. 8. Simulated vs. theoretical p.d.f. of R_{V2U} for different λ_V.

B. Model Verification

For the purpose of model validity and accuracy verification, the value of λ_U was set to 0.02 (UAV/s) whereas all other input parameter values mentioned in Section VI-A were maintained. Figures 6 through 9 are dedicated to exhibiting the simulated curves for the fundamental model parameters and metrics together with their theoretical counterparts. For instance, Figures 6(a) through 6(b) concurrently plot the simulated c.d.f.s of N_A together with their theoretical counterparts for the different values of $\lambda_V \in \{0.1; 0.15; 0.2; 0.25\}$ (Veh/s). These curves almost perfectly overlap and, hence, constitute a tangible proof of the validity and accuracy of the derived formula given in Equation (18). Note that this is the case of all other similar curves generated for $\lambda_V \in [0.1; 0.2777]$ (Veh/s). Due to space limitation, only these sample curves were reported to validate Equation (18) for light, medium and relatively denser ground-bound vehicular traffic. Note that the Mean Squared Error (MSE) between the simulated and theoretical curves has a maximum that is of the order of $10^{-}6$. The same applies for $F_{N_C}(n)$ and $f_{R_{V2U}}(t)$ whose theoretical curves and their simulated counterparts are concurrently plotted in Figures 7(a) through 7(c) and Figures 8(a) through 8(c).

Now, Figures 9(a) through 9(h) concurrently plot the simulated curves pertaining to P_c, (*i.e.* Figure 9(a)) as well as $\overline{R_{V2U}}$, $\overline{N_C}$, $\overline{T_C}$, $\overline{T_D}$, $\overline{T_D^{pc}}$, $\overline{S}$ and $\overline{Q_D}$ (*i.e.*, Figures 9(b) through 9(h)) together with their theoretical counterparts. These figures validate and assert the accuracy of Equations (15), (31), (19), (37), (39), (42) and (43) especially that the minimum and maximum relative differences between the simulated and theoretical curves achieved in all of these plots range respectively from 0% to 2.67%.

C. Performance Evaluation

This subsection evaluates the performance of the considered V2U communication system operating in the context of the networking scenario illustrated in Figure 1. The performance will be evaluated in terms of critical system metrics, namely P_c, $\overline{N_C}$, $\overline{R_{V2U}}$, $\overline{T_C}$, $\overline{T_D}$, $\overline{T_D^{pc}}$, S and $\overline{Q_D}$.

To start with, Figure 9(a) shows that P_c increases as a function of λ_V. Indeed, as λ_V increases, the density of vehicles along the considered roadway increases and, hence, their speed decreases. Under such circumstances, newly arriving UAVs are more likely to catch up and connect with a relatively slowly moving vehicle than with faster ones. This is especially true since a newly arriving UAV is likely to find slowly moving vehicles closer to its arrival point (*i.e.* the entry point to the considered roadway segment) rather than its departure point (*i.e.* the exit point from the considered roadway). Note that P_c shows a rather shy increase as a function of λ_V due to the fact that UAVs have relatively much higher speeds than ground-bound vehicles and, as such, are characterized by a much higher degree of faster mobility allowing them to reach out for

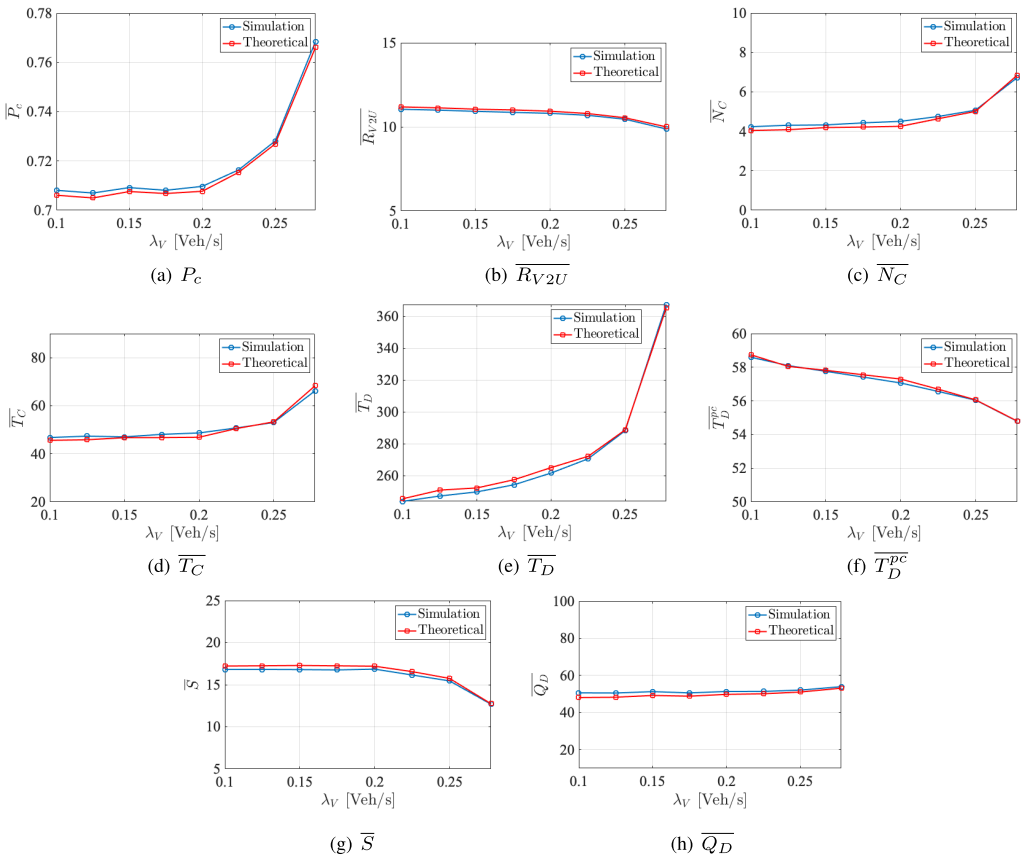

Fig. 9. Simulated vs. theoretical curves of P_c, $\overline{R_{V2U}}$, $\overline{N_C}$, $\overline{T_C}$, $\overline{T_D}$, $\overline{T_D^{pc}}$, $\overline{S}$ and $\overline{Q_D}$ for different λ_V.

far vehicles unless in extreme cases where a newly arriving UAV finds a vehicle that is very close to the roadway's departure point. In this case, no matter how fast the newly arriving UAV is, it has a doubtful ability to reach the vehicle. Now, an increase in P_c translates into an increase in $\overline{N_C}$ since, from the perspective of a global observer monitoring the entire set of turning events will witness more UAVs getting connected to the vehicles. This is shown in Figure 9(c). Nonetheless, unexpectedly, the average per-contact duration, $\overline{R_{V2U}}$ decreases as a function of λ_V. The reason for this can be explained as follows. One has to keep in mind that the UAV traffic is completely independent from the ground-bound vehicular traffic. This being said, the increase in λ_V causes a decrease in ground-bound vehicle speeds (as a result of increasing vehicular density) but has no effect on the UAV speeds. Recall from Equation (21) that, whenever a vehicle-to-UAV contact is established, the per-contact duration is equivalent to the ratio of the vehicle's coverage range to the relative vehicle-to-UAV speed, ΔS. This latter being equal to the difference between the UAV speed and the vehicle speed (refer to Section V-C.3), will increase as a function of λ_V leading, on average, to a decrease in R_{V2U}.

Now, the decrease in $\overline{R_{V2U}}$ is intuitively expected to lead to a decrease in the overall average contact time duration, $\overline{T_C}$. However, as counterintuitively shown in Figure 9(d), $\overline{T_C}$ increases as a function λ_V. This is actually due to the increase in $\overline{N_C}$. Indeed, the slower the vehicles, the more UAVs they are expected to encounter. On the average, this increase in $\overline{N_C}$ overshadows the decrease in $\overline{R_{V2U}}$ causing a net effect being an increase in $\overline{T_C}$. This is expected to bring a decrease in the total average disconnection time $\overline{T_D}$. However, Figure 9(e) shows that $\overline{T_D}$ also increases as a function of λ_V. Indeed, a current UAV that connects to a vehicle at the present time will disconnect from that vehicle at a subsequent time. Hence, since the number of connections increases as a function of λ_V, the number of disconnections will equally increase. However, the average amount of time a vehicle waits until it gets connected again to another subsequently arriving UAV to the roadway is way much larger than the amount of time a connected UAV spends within that vehicle's coverage range. This explains the cumulatively steeper and more significant growth in $\overline{T_D}$ as opposed to its modest $\overline{T_C}$ counterpart. Dividing $\overline{T_D}$ by $\overline{N_C}$ leads to having the per-contact average disconnection period $\overline{T_D^{pc}}$ shown in Figure 9(f) and is self-explanatory. The decrease in the average packet service time, $\overline{S}$, shown in Figure 9(g) is a direct result of the decrease in $\overline{T_D^{pc}}$ since, from Equation (42), $\overline{S}$ is directly proportional to $\overline{T_D^{pc}}$. This decrease in $\overline{S}$ is naturally expected to incur a decrease in the overall average system response time, $\overline{Q_D}$. However, contrary to those expectations, Figure 9(h) shows that $\overline{Q_D}$ is quasi-constant as it just exhibits a very slight increase at high values of λ_V (*i.e.*, $0.2 < \lambda_V \leq 0.2777$) where, it is mostly expected to decrease (since $\overline{S}$ decreases for these values of λ_V). Here, it is worthwhile recalling that as long as a vehicle is connected to a UAV, it keeps on transmitting data to that UAV (*i.e.*, clearing out packets from its OBU's

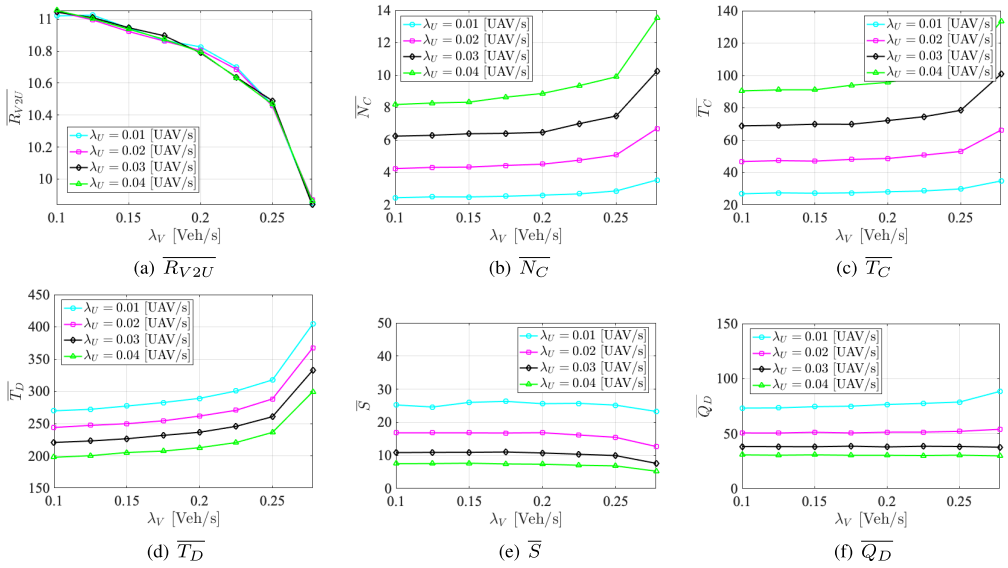

(a) $\overline{R_{V2U}}$ (b) $\overline{N_C}$ (c) $\overline{T_C}$

(d) $\overline{T_D}$ (e) $\overline{S}$ (f) $\overline{Q_D}$

Fig. 10. Variations of $\overline{R_{V2U}}$, $\overline{N_C}$, $\overline{T_C}$, $\overline{T_D}$, $\overline{S}$ and $\overline{Q_D}$ as a function of λ_V and λ_U.

buffer). Hence, here, it becomes obvious that the effect of the vehicle-to-UAV per-contact duration R_{V2U} is implicitly embedded in $\overline{Q_D}$. Indeed, since $\overline{R_{V2U}}$ decreases as a function of the above-mentioned values of λ_V, the number of packets a vehicle is, therefore, able to clear out from its OBU's buffer will be reduced. This implies that the number of packets accumulating in the vehicle's OBU's buffer will increase and, hence, by *Little's Theorem* (refer to [41]), the average queueing delay will increase. This, however, is counteracted by the decrease in $\overline{S}$. Accordingly, over the above-mentioned region of λ_V, $\overline{R_{V2U}}$ and $\overline{S}$ act as two opposing forces that tend to cancel each other. However, the decrease in $\overline{S}$ is slightly steeper than the decrease in $\overline{R_{V2U}}$. This explains the slight increase in $\overline{Q_D}$.

D. Further Discussions

This sub-section is dedicated to providing the reader with further insights into the performance of the V2U communication system in terms of the principle metrics $\overline{R_{V2U}}$, $\overline{N_C}$, $\overline{T_C}$, $\overline{T_D}$, $\overline{S}$ and $\overline{Q_D}$ whenever the UAV arrival rate, λ_U, is varied in the range $[0.01; 0.04]$ (UAVs/s). The behavioral curves pertaining to all of the above-mentioned metrics are plotted as functions of both λ_V and λ_U respectively in Figures 10(a) through 10(f).

To start with, it is important to keep in mind that, as proven in [35], an increase in λ_U directly maps into an increase in the UAV density throughout the aerial field spanning the considered roadway segment. Consequently, the connectivity probability will increase and, hence, $\overline{N_C}$ increases as a function of λ_U as shown in Figure 10(b). In line with such an increase goes the increase in $\overline{T_C}$ as shown in Figure 10(c) as well as the decrease in $\overline{T_D}$ which is illustrated in Figure 10(d). However, for all values of λ_U the behavior of $\overline{R_{V2U}}$ remains the same. This is especially true since the only parameters that have an impact on $\overline{R_{V2U}}$ are the UAV and vehicles speeds, which, here, follow identical distributions drawn over equal ranges for all values of λ_U.

Now, the packet service time will, obviously, decrease as a result of the decrease in $\overline{T_D}$ and the increase in $\overline{N_C}$ (leading to an inevitable decrease in their ratio, which is equivalent to $\overline{T_D^{pc}}$). Finally, the increase in the connectivity probability and $\overline{N_C}$ are directly mapped into the increased likelihood of a vehicle finding itself connected to a UAV and, hence, clearing out more data packets from its OBU's buffer to that UAV. As a result the number of packets in that vehicle's OBU's buffer will decrease causing, together with the decrease in $\overline{S}$, a decrease in the overall system's response time, $\overline{Q_D}$.

VII. Conclusion

This paper considers the opportunistic exploitation of UAVs as a mean to bringing digital connectivity to ground-bound vehicles navigating in isolated dark areas. In this context, a mathematical framework is presented with the objective of capturing the dynamics of the V2U communication system and characterizing its performance in terms of the achievable system's response time. The UAV and ground-bound vehicle mobility models constitute two fundamental building blocks of the established analytical framework herein. This is especially true since the mobility characteristics (*e.g.*, flow rate and speed) of UAVs and ground-bound vehicles are integral components of the vehicle-to-UAV contact durations (*i.e.* the durations during which vehicles are connected to UAVs and, hence, may clear out data packets accumulated within their OBU's buffers). Simulations are conducted to verify the validity and accuracy of the mathematically derived formulas as well as to evaluate the system's performance in scenarios distinguished by UAV availability variations and vehicular densities.

Acknowledgment

The authors would like to acknowledge the financial support that Concordia University and FQRNT have provided for the development of this work.

REFERENCES

[1] D. Orfanus *et al.*, "Self-organization as a supporting paradigm for military UAV relay networks," *IEEE Commun. Lett.*, vol. 20, no. 4, pp. 804–807, Apr. 2016.

[2] M. Mozaffari *et al.*, "Unmanned aerial vehicle with underlaid device-to-device communications: Performance and tradeoffs," *IEEE Trans. Wireless Commun.*, vol. 15, no. 6, pp. 3949–3963, Jun. 2016.

[3] A. Merwaday and I. Guvenc, "UAV assisted heterogeneous networks for public safety communications," in *Proc. WCNCW*, Mar. 2015, pp. 329–334.

[4] Y. Zeng *et al.*, "Wireless communications with unmanned aerial vehicles: Opportunities and challenges," *IEEE Commun. Mag.*, vol. 54, no. 5, pp. 36–42, May 2016.

[5] M. Mozaffari *et al.*, "Mobile unmanned aerial vehicles (UAVs) for energy-efficient Internet of Things communications," *IEEE Trans. Wireless Commun.*, vol. 16, no. 11, pp. 7574–7589, Nov. 2017.

[6] E. Kalantari *et al.*, "On the number and 3D placement of drone base stations in wireless cellular networks," in *Proc. IEEE VTC*, Sep. 2016, pp. 1–6.

[7] I. Bor-Yaliniz and H. Yanikomeroglu, "The new frontier in ran heterogeneity: Multi-tier drone-cells," *IEEE Commun. Mag.*, vol. 54, no. 11, pp. 48–55, Nov. 2016.

[8] M. Mozaffari *et al.*, "Efficient deployment of multiple unmanned aerial vehicles for optimal wireless coverage," *IEEE Commun. Lett.*, vol. 20, no. 8, pp. 1647–1650, Aug. 2016.

[9] *Project Loon*. [Online]. Available: https://www.google.com/intl/es419/loon/how/

[10] S. Black. *UAVs May Deliver Internet Access*. Composites World. [Online]. Available: https://www.compositesworld.com/blog/post/uavs-may-deliver-internet-access

[11] *Airbus Zephyr*. [Online]. Available: https://www.airbus.com/defence/uav/zephyr.html

[12] *Volvo Cars and Ericsson Developing Intelligent Media Streaming For Self-Driving Cars*, document 172080, Volvo Car Group Global Newsroom, 2016.

[13] R. I. Meneguette *et al.*, "A seamless flow mobility management architecture for vehicular communication networks," *J. Commun. Netw.*, vol. 15, no. 2, pp. 207–216, Apr. 2013.

[14] C.-L. Lee *et al.*, "Impact of vehicular networks on emergency medical services in urban areas," *Int. J. Environ. Res. Public Health*, vol. 11, no. 11, pp. 11348–11370, Oct. 2014, doi: 10.3390/ijerph111111348.

[15] S. R. E. Datondji *et al.*, "A survey of vision-based traffic monitoring of road intersections," *IEEE Trans. Intell. Transp. Syst.*, vol. 17, no. 10, pp. 2681–2698, Oct. 2016.

[16] W. Xu *et al.*, "Internet of vehicles in big data era," *IEEE/CAA J. Autom. Sinica*, vol. 5, no. 1, pp. 19–35, Jan. 2018.

[17] J. Joshi *et al.*, "CVMS: Cloud based vehicle monitoring system in VANETs," in *Proc. ICCVE*, 2015, pp. 106–111.

[18] H. Menouar *et al.*, "UAV-enabled intelligent transportation systems for the smart city: Applications and challenges," *IEEE Commun. Mag.*, vol. 55, no. 3, pp. 22–28, Mar. 2017.

[19] Y. Zhou *et al.*, "Multi-UAV-aided networks: Aerial-ground cooperative vehicular networking architecture," *IEEE Veh. Technol. Mag.*, vol. 10, no. 4, pp. 36–44, Dec. 2015.

[20] D. W. Matolak and R. Sun, "Unmanned aircraft systems: Air-ground channel characterization for future applications," *IEEE Veh. Technol. Mag.*, vol. 10, no. 2, pp. 79–85, Jun. 2015.

[21] M. Mozaffari *et al.*, "A tutorial on UAVs for wireless networks: Applications, challenges, and open problems," 2018, *arXiv:1803.00680*. [Online]. Available: https://arxiv.org/abs/1803.00680

[22] W. Khawaja *et al.*, "A survey of air-to-ground propagation channel modeling for unmanned aerial vehicles," *IEEE Commun. Survey Tuts.*, vol. 21, no. 3, pp. 2361–2391, 3rd Quart., 2019.

[23] H. Ghazzai *et al.*, "Data routing challenges in UAV-assisted vehicular ad hoc networks," in *Proc. IARIA Veh.*, France, U.K., 2017.

[24] M. Samir *et al.*, "Joint optimization of UAV trajectory and radio resource allocation for drive-Thru vehicular networks," in *Proc. WCNC*, Marrakesh, Morocco, Apr. 2019, pp. 1–6.

[25] O. S. Oubbati *et al.*, "Intelligent UAV-assisted routing protocol for urban VANETs," *Comput. Commun.*, vol. 107, pp. 93–111, Jul. 2017.

[26] O. S. Oubbati *et al.*, "UAV-assisted supporting services connectivity in urban VANETs," *IEEE Trans. Veh. Technol.*, vol. 68, no. 4, pp. 3944–3951, Apr. 2019.

[27] W. Fawaz *et al.*, "Unmanned aerial vehicles as store-carry-forward nodes for vehicular networks," *IEEE Access*, vol. 5, pp. 23710–23718, 2017.

[28] H. Ghazzai *et al.*, "On the placement of UAV docking stations for future intelligent transportation systems," in *Proc. IEEE VTC*, Jun. 2017, pp. 1–6.

[29] A. Al-Hourani *et al.*, "Optimal LAP altitude for maximum coverage," *IEEE Wireless Commun. Lett.*, vol. 3, no. 6, pp. 569–572, Dec. 2014.

[30] W. Fawaz *et al.*, "UAV-aided cooperation for FSO communication systems," *IEEE Commun. Mag.*, vol. 56, no. 1, pp. 70–75, Jan. 2018.

[31] L. Wang *et al.*, "Multiple access MmWave design for UAV-aided 5G communications," *IEEE Wireless Commun.*, vol. 26, no. 1, pp. 64–71, Feb. 2019.

[32] Telematics Wire. *Ericsson, Orange and PSA Group Partner on 5G Connected Car*. [Online]. Available: http://telematicswire.net/ericsson-orange-psa-group-partner-on-5g-connected-car/

[33] M. Samir *et al.*, "Trajectory planning and resource allocation of multiple UAVs for data delivery in vehicular networks," *IEEE Netw. Lett.*, vol. 1, no. 3, pp. 107–110, Sep. 2019.

[34] M. Khabbaz, "Modelling and delay analysis of intermittently connected roadside communication networks," Ph.D. dissertation, Concordia Univ., Montreal, QC, Canada, Jun. 2012.

[35] M. Khabbaz *et al.*, "Modeling and performance analysis of UAV-assisted vehicular networks," *IEEE Trans. Veh. Technol.*, vol. 68, no. 9, pp. 8384–8396, Sep. 2019, doi: 10.1109/tvt.2019.2911986.

[36] R. Atallah *et al.*, "Multihop V2I communications: A feasibility study, modeling, and performance analysis," *IEEE Trans. Veh. Technol.*, vol. 66, no. 3, pp. 2801–2810, Mar. 2017.

[37] M. Khabazian *et al.*, "Performance modeling of message dissemination in vehicular ad hoc networks with priority," *IEEE J. Sel. Areas Commun.*, vol. 29, no. 1, pp. 61–71, Jan. 2011.

[38] M. Khabazian and M. Ali, "A performance modeling of connectivity in vehicular ad hoc networks," *IEEE Trans. Veh. Technol.*, vol. 57, no. 4, pp. 2440–2450, Jul. 2008.

[39] S. Yousefi *et al.*, "Analytical model for connectivity in vehicular ad hoc networks," *IEEE Trans. Veh. Technol.*, vol. 57, no. 6, pp. 3341–3356, Nov. 2008.

[40] O. Bouachir *et al.*, "A mobility model for UAV ad hoc network," in *Proc. ICUAS*, 2014, pp. 383–388.

[41] L. Kleinrock, *Queueing Systems: Theory*, vol. 1. Hoboken, NJ, USA: Wiley, 1975.

[42] D. Krajzewicz *et al.*, "Recent development and applications of SUMO-Simulation of Urban MObility," *Int. J. Adv. Syst. Meas.*, vol. 5, nos. 3–4, 2012.